

Full down-conversion of amber-emitting phosphor-converted light-emitting diodes with powder phosphors and a long-wave pass filter

Jeong Rok Oh,^{1,4} Sang-Hwan Cho,^{2,4} Hoo Keun Park,¹ Ji Hye Oh,¹ Yong-Hee Lee,³ and Young Rag Do^{1,*}

¹Department of Chemistry, Kookmin University, Seoul 136-702, Korea

²Department of Physics, KAIST, Daejeon 305-701, Korea

³Department of Physics and Graduate School of Nanoscience & Technology (World Class University), KAIST, Daejeon 305-701, Korea

⁴These authors contributed equally to this work.

*yrdo@kookmin.ac.kr

Abstract: This paper reports the possibility of a facile optical structure to realize a highly efficient monochromatic amber-emitting light-emitting diode (LED) using a powder-based phosphor-converted LED combined with a long-wave pass filter (LWPF). The capping of a blue-reflecting and amber-passing LWPF enhances both the amber emission from the silicate amber phosphor layer and the color purity due to the blocking and recycling of the pumping blue light from the InGaN LED. The enhancement of the luminous efficacy of the amber pc-LED with a LWPF (phosphor concentration 20 wt%, 39.4 lm/W) is 34% over that of an amber pc-LED without a LWPF (phosphor concentration 55 wt%, 29.4 lm/W) at 100 mA and a high color purity (> 96%) with Commission International d'Eclairage (CIE) color coordinates of $x = 0.57$ and $y = 0.42$.

© 2010 Optical Society of America

OCIS codes: (220.0220) Optical design and fabrication; (230.0230) Optical devices; (230.1480) Bragg reflectors; (230.3670) Light-emitting diodes.

References and links

1. M. Yamada, T. Naitou, K. Izuno, H. Tamaki, Y. Murazaki, M. Kameshima, and T. Mukai, "Red-enhanced white-light-emitting diode using a new red phosphor," *Jpn. J. Appl. Phys.* **42**(Part 2, No.1A/B), L20–L23 (2003).
2. R. Mueller-Mach, G. O. Mueller, M. R. Krames, H. A. Höpfe, F. Stadler, W. Schnick, T. Juestel, and P. Schmidt, "Highly efficient all-nitride phosphor-converted white light emitting diode," *Phys. Status Solidi A* **202**(9), 1727–1732 (2005).
3. K. Uheda, N. Hirosaki, Y. Yamamoto, A. Nanito, T. Nankajima, and H. Yamamoto, "Luminescence properties of a red phosphor, $\text{CaAlSiN}_3:\text{Eu}^{2+}$, for white light-emitting diodes," *Electrochem. Solid-State Lett.* **9**(4), H22–H25 (2006).
4. Y. Sato, N. Takahashi, and S. Sato, "Full-color fluorescent display devices using a Near-UV light-emitting diode," *Jpn. J. Appl. Phys.* **35**(Part 2, No. 7A), L838–L839 (1996).
5. Y. D. Huh, J. H. Shim, Y. Kim, and Y. R. Do, "Optical properties of three-band white light emitting diodes," *J. Electrochem. Soc.* **150**(2), H57–H60 (2003).
6. R. Mueller-Mach, G. O. Mueller, M. R. Krames, and T. Trottier, "High-Power Phosphor-Converted Light-Emitting Diodes Based on III-Nitrides," *IEEE J. Sel. Top. Quantum Electron.* **8**(2), 339–345 (2002).
7. R. Mueller-Mach, G. O. Mueller, M. R. Krames, O. B. Shchekin, P. J. Schmidt, H. Bechtel, C.-H. Chen, and O. Steigelman, "All-nitride monochromatic amber-emitting phosphor-converted light-emitting diodes," *Phys. Status Solidi RRL* **3**(7-8), 215–217 (2009).
8. M. Peter, A. Laubsch, W. Bergbauer, T. Meyer, M. Sabathil, J. Baur, and B. Hahn, "New developments in green LEDs," *Phys. Status Solidi A* **206**(6), 1125–1129 (2009).
9. J. M. Phillips, M. E. Coltrin, M. H. Crawford, A. J. Fisher, M. R. Krames, R. Mueller-Mach, G. O. Mueller, Y. Ohno, L. E. S. Rohwer, J. A. Simmons, and J. Y. Tsao, "Research challenge to ultra-efficient inorganic solid-state lighting," *Laser Photon. Rev.* **1**(4), 307–333 (2007).
10. J.-Y. Chi, J.-S. Chen, C.-Y. Liu, C.-W. Chu, and K.-H. Chiang, "Phosphor converted LEDs with omnidirectional-reflector coating," *Opt. Express* **17**(26), 23530–23535 (2009).
11. J. R. Oh, S.-H. Cho, Y.-H. Lee, and Y. R. Do, "Enhanced forward efficiency of $\text{Y}_3\text{Al}_5\text{O}_{12}:\text{Ce}^{3+}$ phosphor from white light-emitting diodes using blue-pass yellow-reflection filter," *Opt. Express* **17**(9), 7450–7457 (2009).

12. S.-H. Cho, J. R. Oh, H. K. Park, H. K. Kim, Y.-H. Lee, J.-G. Lee, and Y. R. Do, "Highly efficient phosphor-converted white organic light-emitting diodes with moderate microcavity and light-recycling filters," *Opt. Express* **18**(2), 1099–1104 (2010).
 13. J. K. Park, C. H. Kim, S. H. Park, H. D. Park, and S. Y. Choi, "Application of strontium silicate yellow phosphor for white light-emitting diodes," *Appl. Phys. Lett.* **84**(10), 1647–1649 (2004).
 14. H. A. Macleod, *Thin-Film Optical Filters* 3rd Edition (Institute of Physics Publishing, 2003).
 15. W. Schnick, "Shine a light with nitrides," *Phys. Status Solidi RRL* **3**(7-8), A113–A114 (2009).
 16. C.-H. Kuo, J.-K. Sheu, S.-J. Chang, Y.-K. Su, L.-W. Wu, J.-M. Tsai, C. H. Liu, and R. K. Wu, "n-UV+Blue/Green/Red white light emitting diode lamps," *Jpn. J. Appl. Phys.* **42**(Part 1, No. 4B), 2284–2287 (2003).
-

1. Introduction

Technologies for achieving high-efficiency and high color rendering index (CRI) white phosphor-converted light-emitting diodes (pc-LEDs) have been studied actively in recent years for solid-state lighting applications. Generally, pc-LED methods to obtain white emission involve the mixing of the unabsorbed blue emission from a blue AlGaInN-based LED and the down-converted yellow or green/red emissions from phosphors [1–5]. At present, this 'partial' down-conversion concept of using color conversion phosphors in combination with blue LEDs has been widely adopted in lightning and display devices. Otherwise, it is rarely discussed in relation to producing monochromatic or high-color-purity light from pc-LEDs [5,6]. However, very recently, the 'full' down-conversion approach was presented by Muller-Mach et al. in a study that realized a highly efficient amber-emitting all-nitride pc-LED [2]. They produced a high-color-purity (>96%) amber pc-LED to overcome the low efficiency problem of direct amber-emitting LEDs when used with high-color-purity (Ba,Sr)₂Si₅N₈:Eu²⁺ phosphor (>98%). When producing colored light from the full down-conversion of a pc-LED, it is important to match the light and optical properties to the requirements of the user.

Typically, amber LEDs are used in automobile applications or in traffic signals. Furthermore, amber LEDs are promising as an illumination light source for photolithography rooms because the absence of blue LEDs protect photoresists from exposure under illumination.

Although it is possible to obtain a full spectrum of colors from III-V-based LEDs and related compounds, it appears to be difficult to achieve reasonable efficiency for emission in the deep green to amber region of spectrum between 510–610 nm. This is well known as the "green window" or "yellow gap" problem [7–9], and it impedes the use of efficient amber color from a direct emissive LED for applications as indicators in automobiles or traffic signals. Hence, Muller-Mach et al. initiated the 'full' down-conversion approach to solve a problem with low LED performance at wavelengths in the yellow gap region [7]. Simultaneously, they used a densely sintered translucent ceramic of (Ba,Sr)₂Si₅N₈:Eu amber phosphor to overcome the scattering problem in a powder-based phosphor system. Although they pioneered an innovative approach to produce highly effective monochromatic light from pc-LEDs for general lighting applications, all types of phosphors cannot be sintered easily into highly efficient ceramic phosphors. Furthermore, pc-LEDs coated with powder-based phosphors remain the dominant technology in current lighting applications, as easy control of the coating process is technically acceptable during the packaging process of pc-LEDs. Meanwhile, very recently, Chi et al. introduced an omnidirectional-reflective (ODR) coating on white LED combined with red, green, blue phosphor and UV LED to recycle and block the UV light from the LED chip [10]. With this approach, they obtained a highly efficient white LED based on the recycling of UV light.

At present, the ODR approach allows the proposal of a simple and facile idea to realize amber light pc-LEDs using powder phosphors in association with a blue-mirror-yellow-pass filter.

In a conventional approach for obtaining monochromatic phosphor color using blue-excited pc-LEDs coated with powder-based phosphors, the phosphor layer should be thick and highly concentrated to block the unabsorbed blue emission from the pc-LED. This approach is hampered by the low phosphor conversion efficiency due to the additional scattering

associated with the high concentration of the phosphor content in the paste. Instead of increasing the phosphor content, a long-wave pass filter (LWPF) is introduced here on top of a silicate ((Sr,Ba,Ca)₃SiO₅:Eu) amber phosphor-coated InGaN-based LED die to block and recycle unabsorbed transmitted blue emission. This LWPF functions as a mirror for blue LED light and as a window for the amber phosphor emission. This approach stands on contrast with the concept of a short-wave pass filter (SWPF, also known as a light-recycling filter (LRF)) which recycles the backward emission of the phosphor layer into the blue LED, as previously reported by the authors [11,12]. Therefore, the present paper reports the possibility of a facile optical structure to realize a highly efficient monochromatic amber-emitting pc-LED using a powder-based amber pc-LED combined with a LWPF. In addition, the blocking and recycling capability of three different types of LWPFs from unabsorbed transmitted blue emission is assessed with the concentration of the amber phosphor powders in the paste.

2. Experimental methods

To examine the effect of the LWPFs experimentally, three types (A1, A2 and A3) of dielectric LWPFs were fabricated on glass substrates. For the fabrication of the LWPF stacks, terminal eighth-wave thick TiO₂ (A1: 23 nm, A2: 24 nm, A3: 25 nm) and quarter-wave thick SiO₂/TiO₂ (A1: 69/46 nm, A2: 72/48 nm, A3: 73/50 nm) films were coated onto a glass substrate by e-beam evaporation at 250°C. The base pressure in the e-beam chamber was fixed at 4.0×10^{-5} torr. The deposition was performed at an acceleration voltage of 7 kV with an oxygen partial pressure of 1.9×10^{-4} torr. Three different types of LWPFs were deposited on glass substrates with different thicknesses for the TiO₂ and SiO₂, as summarized in Table 1.

Table 1. The thickness of the three types of LWPF multi-layer stacks

Layer	Thickness (nm)		
	A1	A2	A3
0.5H	23	24	25
L	69	72	73
0.5H	23	24	25

The refractive indices (n) and extinction coefficients (k) of the e-beam evaporated SiO₂ and TiO₂ films were measured using a spectroscopic ellipsometer (Sentech, SE800). The detailed wavelength dispersion of the n and k values of the as-grown SiO₂ and TiO₂ films were reported previously by the authors [11]. These measured n and k values were used to simulate the reflectance (R), transmittance (T), and absorption (A) in the design of the three types of LWPFs.

To fabricate the pc-LEDs, a blue chip ($\lambda_{\max} = 455$ nm) was used simultaneously as a blue light source and an excitation source for the amber phosphor. Silicate ((Sr,Ba,Ca)₃SiO₅:Eu) amber powder phosphors were also used in this experiment. (Sr,Ba,Ca)₃SiO₅:Eu amber phosphors were synthesized through a solid state reaction. The synthetic procedures followed the procedures detailed in a previous publication by Park et al. [13]. The emission color of (Sr,Ba,Ca)₃SiO₅:Eu can be tuned by the Ba/Sr/Ca ratio and the Eu doping concentration over a wide range of colors. Various amounts of amber phosphors (5, 10, 15, 20, 25, 30, 35, 40, 45, 50, 55, and 60 wt%) were dispersed in a silicone binder, and the same amounts of resulting phosphor pastes were dropped onto a cup-type blue chip to make the pc-LEDs. On top of the various amber pc-LEDs, a LWPF-coated glass substrate was attached with an air gap.

The forward emissions of the emission spectra from the conventional blue LED, blue-excited pc-LEDs and blue-excited pc-LEDs with the LWPF-coated glass substrates were measured in an integrated sphere using a spectrophotometer (PSI Co. Ltd., Darsar). Luminous efficacy and quantum efficiency are defined as the brightness and integrated emission spectra of both the (Sr,Ba,Ca)₃SiO₅:Eu-coated conventional and LWPF-assisted LEDs, respectively, at a constant current or power. The external efficiency and color purity of the three types of LWPF-coated amber pc-LEDs were compared with the current at various phosphor

concentrations. The thicknesses and structures of the LWPF were measured with a field-emission scanning electron microscope (FESEM) (JSM 7401F, JEOL) operated at 10 kV.

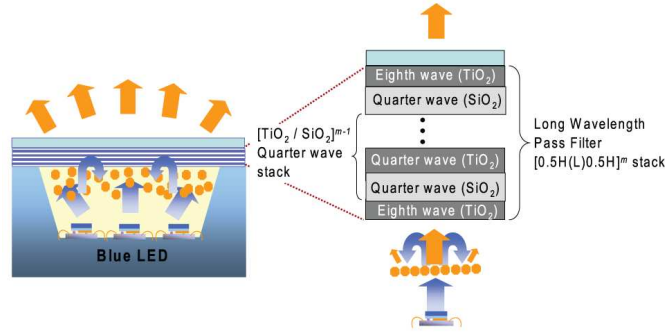


Fig. 1. Schematic diagram of the silicate amber phosphor-coated LED device structure with the embedded amber light passing through and blue light reflecting from the dielectric multilayer coated glass substrate. The enlarged side view shows the mechanism of the enhancement of the forward emission from the amber phosphor layer and the basic sequence of the modified quarter-wave stacks of the LWPF.

3. Results and discussion

Figure 1 shows a schematic diagram of the silicate amber phosphor-coated LED die covered with the LWPF multilayer coated glass substrate. This figure shows the mechanism of the backward reflection from the forward unabsorbed emission of blue LED into the amber phosphor-coated LED die. The high transmission of the LWPF stacks at the amber wavelength allow the most of emitted amber light in the escape cone to pass through the LWPF-assisted substrate. In addition, the high reflectance band of the LWPF stacks at the blue wavelength can block the transmission of blue and redirect the unabsorbed blue light to the amber phosphor layer coated onto the LED die/cup if a large amount of blue light passes through phosphor layer. Therefore, the full conversion of the forward emission from the amber phosphors of the LWPF covered pc-LED die is due to the high reflection and re-excitation of unabsorbed blue light from the LED into the amber phosphors as well as to the high transmission of the forward emission of the phosphors.

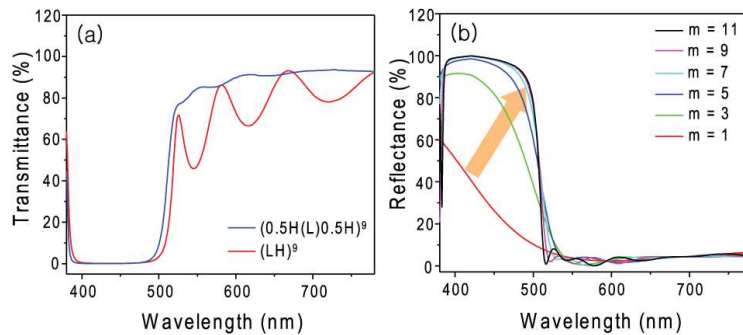


Fig. 2. (a) Comparison of the simulated transmittance of a conventional LWPF (Red line) and the modified LWPF (blue line). (b) Comparison of the simulated reflectance of the modified LWPF with different numbers of $[0.5H(L)0.5H]^m$ stacks.

For the design of the LWPF multilayer films for the blue-excited pc-LEDs, the characteristic matrix method was used to simulate the reflectance (R), transmittance (T), and absorption (A) of the optical structure of LRF stacks [11,12,14]. As previously reported for an omnidirectional-reflective (ODR) filter for near UV-excited pc-LEDs [10], a conventional quarter-wave film of alternating high- and low-refractive index dielectric films is considered

to be a candidate for LWPF dielectric stacks for blue-excited pc-LEDs. However, a conventional quarter-wave film shows stronger interference oscillations of its transmission peaks in the long wavelength region, as determined in the simulations [see Fig. 2(a)]. This can decrease the transmission of emission light from the phosphor layer. In this study, a stack of modified quarter-wave films is proposed as a good candidate for a LWPF substrate. The simulated spectra also indicate that the modified stacks used here are more transparent of transmitted light in the amber region compared to conventional quarter-wave stacks. The basic sequence of the modified quarter-wave stacks for LWPF used in this study is shown in the inset of Fig. 1. This sequence simply entails the addition of a pair of eighth-wave layers of high-index layers to the quarter wave stack, one at each end, as delineated by the following formula.

$$G[0.5H(L)0.5H]^m A$$

Here, the combination 0.5H(L)0.5H (eighth-wave high-index TiO₂ (0.5H) and quarter-wave low-index SiO₂ (L); 0.5TiO₂(SiO₂)0.5TiO₂) between the glass substrate G and air A is repeated m times. As shown in the simulation results in Fig. 2(b), the reflectance at the blue region increased as the periodic number of stacks was increased to m = 9, becoming saturated above m = 9. Meanwhile, the long-wavelength edge of the reflectance band was tuned by controlling the basic period of the dichroic multilayer. In the simulation, the thicknesses of the high-index (TiO₂) and low-index (SiO₂) films were varied to tune the spectral position of the reflectance band. In this publication, we fabricated three different types of LWPFs with m = 9 (A1 = 503, A2 = 517 nm and A3 = 527 nm at band-edge of long-wavelength) as capping filters to analyze the effect of LWPF films on the forward emission of pc-LEDs with (Sr,Ba,Ca)₃SiO₅:Eu silicate powder-based amber phosphors.

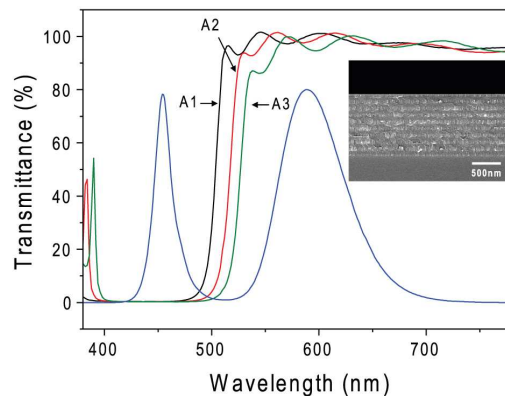


Fig. 3. Measured transmittance spectra of the three different LWPFs [0.5H(L)0.5H]⁹ (L: low index layer, SiO₂, H: high index layer, TiO₂) on glass substrates, and the normalized electroluminescent (EL) spectrum of pc-LED with silicate amber powder phosphor (phosphor concentration 20 wt%). The inset shows a side-view scanning electron microscopy (SEM) image of the nine periods of the [0.5H(L)0.5H] films coated onto a glass substrate.

The inset in Fig. 3 shows a side-view scanning electron microscopy (SEM) image of an actual fabricated A3-LWPF dielectric multilayer comprised of modified, alternate TiO₂ and SiO₂ quarter-wave films of the nine periods. This image indicates that the thicknesses of the obtained TiO₂/SiO₂ films satisfactorily match those of the dielectric films in the designed LWPFs. The measured transmittance spectra of the three different types of short-wavelength mirrors and long-wavelength windows are shown in Fig. 3. The long-wavelength edge of the high-reflectance band shifts toward a greenish color with an increase in the lattice parameter of the nine periods of the modified quarter-wave films. This figure also compares the transmittance spectra of three LWPFs and the normalized EL spectrum of a pc-LED with silicate amber phosphors. The figure clearly indicates that the emission band of the blue-

excited pc-LED at a shorter wavelength can be overlapped with the reflection bands of the LWFs at shorter wavelength. Otherwise, the transmittance of the blue-excited pc-LED at the amber region is maintained in excess of 90%, as the overlap between the emission band and the reflectance band is minimized.

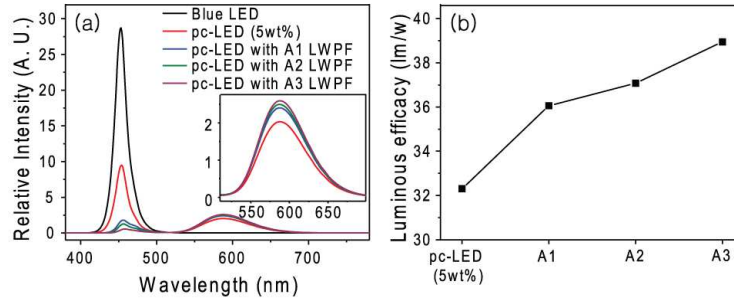


Fig. 4. (a) The equal-power spectra of a conventional blue-pumped pc-LED and pc-LEDs with three types of LWFs (phosphor concentration: 5 wt%). The enlarged view shows the spectra at the amber region. The black line shows the spectra of only the conventional blue LED. (b) The luminous efficacy of pc-LEDs (5 wt%) of a conventional blue-pumped pc-LED and pc-LEDs with three types of LWFs.

The forward emission spectrum, external efficiency, brightness and color purity of the three types of LWPf capped pc-LEDs were compared with various phosphor concentrations. Figure 4(a) shows the equal-power emission spectra of a conventional blue-pumped silicate phosphor pc-LED and three LWPf multilayer-assisted silicate pc-LEDs at the integrated sphere. All of the samples have the same phosphor concentration of 5 wt% in a silicone matrix. Here, the vertical output spectrum is the sum of the non-absorbed blue light and the forward phosphor emissions. The LWPf capped pc-LEDs showed much weaker intensities than the conventional pc-LED at the blue LED emission wavelength and slightly higher intensity than that of a conventional pc-LED at the amber phosphor emission wavelength. The intensity at the amber emission region is the highest in the A3 LWPf case. Figure 4(b) also clearly indicates that the A3 filter enhances the luminous efficacy of pc-LED more than the A1 and A2 LWPf. Here, we performed further variation experiments using pc-LEDs with A3 LWPf.

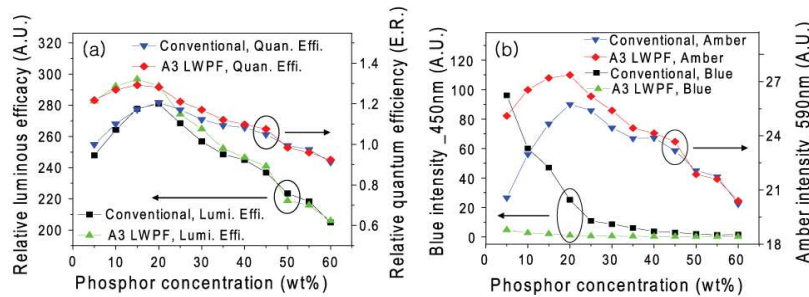


Fig. 5. (a) The relative luminous efficacies and the relative quantum efficiencies of the conventional pc-LED and pc-LED with A3 LWPf as a function of the phosphor concentration in paste. (b) The relative blue and amber intensities of the emission spectra of the conventional pc-LED and pc-LED with A3 LWPf as a function of the phosphor concentration. All measurements were performed under equal-current (100 mA).

Figure 5(a) shows the relative luminous efficacy and the relative quantum efficiency of the conventional and A3 LWPf pc-LED as a function of the phosphor concentration. The relative quantum efficiency is defined as 1.0 when the condition of the phosphor concentration of the conventional pc-LED is 5.0 wt%. As the phosphor concentration increases, the enhancements of luminous efficacy and quantum efficiency from the A3 LWPf pc-LED compared to the

conventional pc-LED decrease. This occurs for the following reason. As the phosphor concentration increases, the thickness of the phosphor layer becomes thicker. Accordingly, the blue light is mostly blocked and is scattered and absorbed at the phosphor layer. As a result, the enhancement resulting from the recycled blue light is reduced. Figure 5(b) shows the relative intensities of the transmitted blue and amber light of the conventional and the A3 LWPF pc-LED as a function of the phosphor concentration. The amber intensity is highest at the phosphor concentration 20 wt %. For the conventional pc-LED, a large amount of blue pumping light from the blue LED source is transmitted forward at a low phosphor concentration. However, in the case of the A3 LWPF pc-LED, the blue light is blocked by the LWPF stack due to high reflectance band at the blue wavelength. In addition, the reflected blue light contributes to re-excitation at the amber phosphor layer. Hence, the amber intensity of the LWPF capped pc-LED is enhanced.

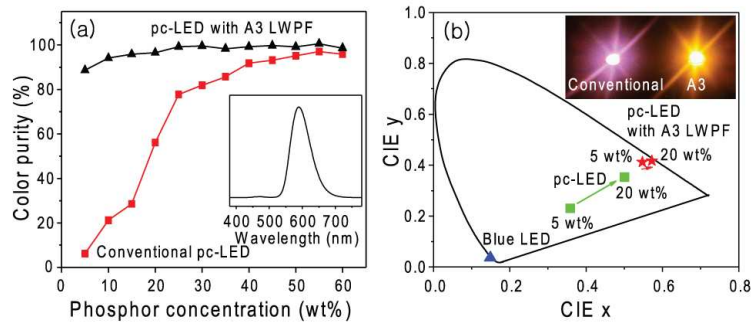


Fig. 6. (a) Comparison of the color purity of an silicate pc-LED with and without LWPF A3 as a function of the phosphor concentration. The inset shows the EL spectrum of the A3 LWPF capped powder-based silicate pc-LED (20 wt %). (b) 1931 CIE color coordinates of a pc-LED without a LWPF (squares) and a pc-LED with A3 LWPF (stars) as a function of the phosphor concentration (5 wt% - 20 wt%). The inset shows an image of the pc-LED without a LWPF (left) and with a LWPF (right). All measurements were performed under equal-current (100 mA).

The color purities of both pc LEDs with a LWPF and without a LWPF are shown in Fig. 6(a). In this case, the color purity of the pc-LED with A3 is greater than 90% at all phosphor concentrations and greater than 96% at the phosphor concentration of 20 wt %. The phosphor concentration should reach 55 wt% to obtain high color purity that exceeds 96% for a pc-LED without a LWPF. Therefore, we emphasize that the use of a powder-based amber pc-LED can lead to high color purity at a low phosphor concentration when using the proposed LWPF. As shown in Fig. 5(a) and 6(a), the capping of the A3 LWPF on the top of the silicate pc-LED (20 wt% phosphor concentration) resulted in a 1.25 fold increase in the relative luminous efficacy of the forward amber emission compared to that of a silicate pc-LED without a LWPF (55 wt% phosphor concentration) at equal-current (100 mA) and at a similar color purity. The emission spectrum of the A3 LWPF capped pc-LED shows a peak maximum wavelength of 590 nm (the inset in Fig. 6 (a)). Figure 6(b) also shows the chromaticity of pc-LEDs as a function of the phosphor concentration. Here, the variations in the pc-LED with a LWPF are very small in comparison to that of the pc-LED without a LWPF. The Commission International d'Eclairage (CIE) 1931 coordinates for a pc-LED with the LWPF A3 in conjunction with 20 wt % silicate powder phosphors are 0.57 and 0.42, values that lie well within the "amber box" of the SAE specifications. Images of the fabricated amber pc-LEDs with and without a LWPF are shown side-by-side in the inset of Fig. 6(b) for comparison. These figures clearly indicate that the full down-conversion of a monochromatic amber LED is realized by simply capping a LWPF onto a powder-based pc-LED, even at a low phosphor concentration in a phosphor paste.

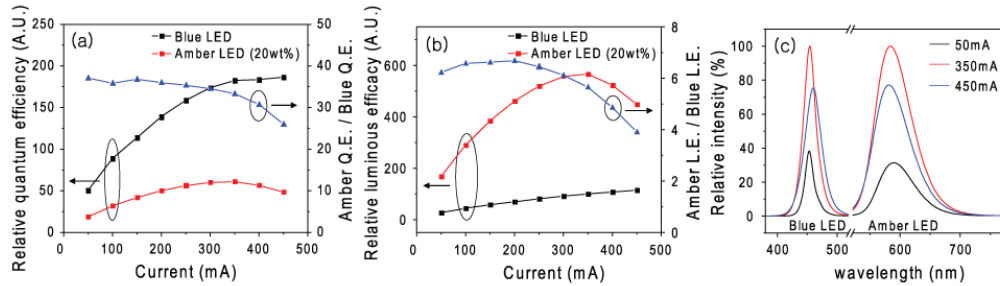


Fig. 7. (a). The relative quantum efficiencies of a conventional blue LED (InGaN LED) and the fabricated amber pc-LED with a LWPF (20 wt%) as a function of the driving current. (b) Comparison of the luminous efficacy of a blue LED and an amber pc-LED with a LWPF as a function of the driving current. (c) Spectra comparing a blue LED and an amber pc-LED as a function of the driving current (50, 350 and 450 mA, dc-operation).

Figures 7(a) and 7(b) show the relative quantum efficiency and the relative luminous efficacy for both a conventional pumping blue LED (InGaN LED) and an amber LED (a pc-LED with an A3 filter at a phosphor concentration 20 wt%) as a function of the driving current. The relative quantum efficiency of the amber pc-LED with the LWPF is 37% of the blue-pumped LED at 100 mA (the regular current of our blue LED is 100 mA) and over 30% with up to 400 mA of current. As previously reported, the maximum external quantum efficiency (EQE), given as the ratio of emitted photons to the injected carriers, of a blue LED has been reported to be approximately ~65% thus far [15]. It can be supposed that the EQE of a silicate-powder-phosphor-based pc-LED with the A3 LWPF is 24% if the most efficient blue LED is used as a pumping LED for the LWPF capped pc-LED. This implies that the EQE of the LWPF capped silicate amber pc-LED remains above the performance of the direct AlGaInP amber LED, as the highest EQE of a direct amber LED was reported to be 11% [7]. Figure 7(b) shows a similar trend in the relationship between the relative luminous efficacy and the current and that of the efficiency and the current. The luminous efficacy of the amber pc-LED with the A3 LWPF is 6.2 times higher than that of a conventional pumping blue LED at 100 mA. These figures also show that the relative luminescence efficiency and luminous efficacy of an amber LWPF pc-LED decrease slightly compared to those of a pumping blue LED as the applied current is increased. This is due to the current saturation and/or the thermal quenching of the silicate amber phosphors, as the current and temperature influence on the performance cannot be separated under direct voltage (dc) operation in this experiment.

The color stability with the driving current, as shown in Fig. 7(c) is excellent for an amber pc-LED with a LWPF. The amber pc-LED with the LWPF shows only small variations in its spectra over all drive dc-current conditions. In contrast, the conventional blue LED (InGaN) does not appear to be as stable. This is due to the general fact that the photoluminescence emission spectra of color-changing powder phosphors are more stable than the electroluminescence emission spectra of the pumping blue InGaN LED under different currents and temperatures [16].

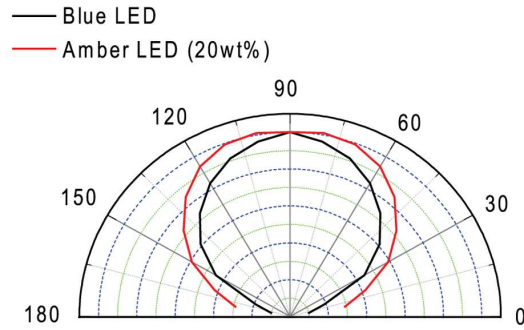


Fig. 8. Comparison of the angular-radiation patterns of the blue LED and the amber pc-LED with the LWPF

Figure 8 plots the normalized luminous efficacy as a function of the viewing angle for the conventional blue LED and amber pc-LED with the LWPF. The luminous efficacies of both LEDs show Lambertian behaviors. Hence, the proposed amber pc-LED with the LWPF clearly shows comparable variations in its angular radiation patterns over a large angular span.

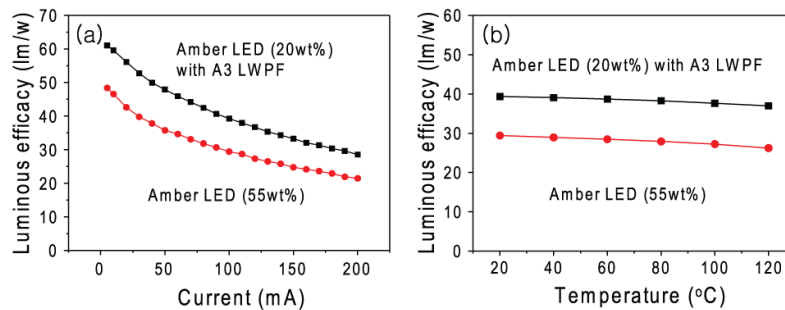


Fig. 9. Comparison of the luminous efficacy of the direct-emitting amber pc-LED (20 wt%) and the amber pc-LED with LWPF (55 wt %) as a function of (a) current density and (b) ambient temperature.

We compare the equal-power luminous efficacy of a full down-conversion pc-LED with A3 LWPF (phosphor concentration, 20 wt%) and that of a full down-conversion direct-emitting pc-LED (phosphor concentration, 55 wt%) as a function of current density and ambient temperature, in order to address the superior optical properties of an LWPF capped pc-LED to those of a direct emitting pc-LED. Figure 9 shows that the luminous efficacy of the amber pc-LED with the LWPF is higher than that of an amber pc-LED without an LWPF over the whole experimental range of current density up to 200 mA and ambient temperature up to 120 °C at a similar color purity level. The luminous efficacy of full down conversion pc-LED with and without LWPF is 39.4 and 29.4 lm/W at 100 mA, respectively. The measured luminous efficacy of the amber pc-LED with the A3 LWPF is 1.34 times higher than that of a direct-emitting amber pc-LED. In addition, both samples also show similar current and temperature dependence of luminous efficacy irrespective of using LWPF. This means that an efficient monochromatic color is realized by the pc-LED using low-concentrated powder-type phosphors with the help of LWPF and that the current and temperature dependence of luminous efficacy of LWPF assisted pc-LEDs depend only on the material type of the phosphor and not on the presence of LWPF.

4. Conclusions

In summary, a highly efficient and high-color purity monochromatic amber pc-LED using a powder-based amber pc-LED combined with a LWPF was proposed and demonstrated. The capping by a blue-reflecting and amber-passing LWPF enhances the amber emission from the

(Sr,Ba,Ca)₃SiO₅:Eu phosphor layer and the color purity due to the blocking and recycling of the pumping blue light. The equal-current and equal-power luminous efficacy of the amber pc-LED with the LWPF (20 wt% phosphor concentration) was enhanced by 25% and 34% over that of an amber pc-LED without an LWPF (55 wt% phosphor concentration) at a similar color purity level (> 96%), respectively. Furthermore, the proposed amber pc-LED with the LWPF provides good drive current, ambient temperature stability and an acceptable viewing-angular tolerance. These results are the first that show the possibility of a monochromatic amber pc-LED using a powder-based method with the help of LWPFs.

Acknowledgements

This study was supported by the Korea Science and Engineering Foundation (Nano R&D program grant # 2008-03573 and ERC program grant # R11-2005-048-00000-0) and a grant (code# F0004100-2008-31) from the Information Display R&D Center, one of the 21st Century Frontier R&D Programs funded by the Ministry of Knowledge Economy of Korea. This work was partially supported by the National Research Foundation through a Korea Grant funded by the Korean Government (MEST) (NRF-C1AAA001-2009-0092938).